ASEAN Journal for Science and Engineering in Materials

Journal homepage: https://ejournal.bumipublikasinusantara.id/index.php/ajsem

Experimental and Numerical Investigation of Hybrid Thin-Walled Aluminum/Glass Fiber-reinforced Polymer Conical Energy Absorbers Filled with Polyurethane Foam under Impact Loading

*Adisak Pawong, Kunanon Sakkampang, Nirut Onsalung**

Rajamangala University of Technology Isan, Sakon Nakhon Campus, Thailand

*Correspondence: E-mail: nirut.on@rmuti.ac.th

ABSTRACT

This study investigated the crashworthiness performance of hybrid thin-walled aluminum/glass fiber-reinforced polymer (GFRP) conical energy absorbers filled with polyurethane foam under axial impact loading. Various cone angles were examined. The specimens consisted of unreinforced aluminum conical tubes, GFRP-reinforced aluminum conical tubes, and GFRP-reinforced aluminum conical tubes filled with polyurethane foam at various densities. Experimental impact testing and finite element analysis (FEA) were conducted to evaluate energy absorption, specific energy absorption, and failure behavior. The AL70/G configuration achieved the best crashworthiness performance, with the highest energy absorption and specific energy absorption. The experimental and FEA results showed similar trends, confirming that cone angle and GFRP reinforcement strongly influenced the impact response of the hybrid conical energy absorbers.

ARTICLE INFO

Article History:

Submitted/Received 23 Jan 2026
First Revised 10 Jul 2026
Accepted 27 Jul 2026
First Available online 10 Aug 2026
Publication Date 01 Dec 2026

Keywords:

Composite material;
Conical energy absorber;
Finite element analysis;
GFRP;
Impact loading;
Polyurethane foam.

p-ISSN: 2828-920X e-ISSN: 2828-9951

1. INTRODUCTION

Lightweight crashworthy structures are essential in modern transportation systems, including automobiles, trains, and aircraft. In vehicle structures, energy-absorbing components are required to reduce impact forces before they are transferred to the passenger compartment. Therefore, the development of structural materials must consider both impact resistance and a high strength-to-weight ratio. Thin-walled metallic structures have been widely investigated for this purpose because they can absorb impact energy through progressive plastic deformation. Previous studies have examined the collapse behavior of square, circular, tapered, and conical metallic tubes under quasi-static and impact loading conditions (Gupta *et al.*, 2008; Zarei and Kröger, 2006).

Thin-walled tubes are commonly used as primary crashworthy components because their geometry can be designed to control deformation and energy absorption. Different cross-sectional shapes, including circular, square, top-hat, double-hat, and conical tubes, have been applied in energy-absorbing structures (Goel, 2015; Qi *et al.*, 2012; Liu *et al.*, 2016). Among these configurations, conical structures are attractive because their tapered geometry can influence collapse behavior, load response, and energy absorption during axial impact. However, the crashworthiness performance of conical structures is strongly affected by geometric parameters, including cone angle, diameter ratio, wall thickness, and reinforcement arrangement.

In addition to metallic structures, composite materials have gained increasing attention for lightweight crashworthy applications. Composite materials consist of matrix and reinforcement phases, which can provide high strength and stiffness while reducing structural weight (Nandiyanto et al., 2022). Glass fiber-reinforced polymer (GFRP) and carbon fiber-reinforced polymer (CFRP) are commonly used in engineering structures because of their favorable mechanical properties and specific strength. The performance of composite structures is influenced by several parameters, including geometry, laminate stacking sequence, fiber orientation, material properties, and impact velocity (Ataabadi *et al.*, 2019; Wu *et al.*, 2023; Wang *et al.*, 2023). In particular, GFRP composites are suitable for crashworthy structures because they provide relatively high strength, good availability, and lower cost compared with carbon fiber composites.

Foam filling is another strategy for improving the impact performance of thin-walled structures. Foam-filled tubes can promote stable collapse, reduce sudden peak load, and improve energy absorption during crushing. Various foam materials have been investigated, including polyurethane foam, aluminum foam, polyvinyl chloride foam, and expanded polystyrene foam (Mirfendereski *et al.*, 2008; Hall *et al.*, 2002; Yalçın and Genel, 2019; Ozturk and Anlas, 2011). Polyurethane foam is particularly attractive because it is lightweight, relatively inexpensive, and capable of supporting progressive deformation in crashworthy structures (Onsalung *et al.*, 2014). Foam-filled structures can improve collapse stability and energy absorption efficiency under impact loading (Gan *et al.*, 2016; Hanssen *et al.*, 2000).

The combination of aluminum, GFRP reinforcement, and polyurethane foam can produce hybrid thin-walled structures with improved crashworthiness performance. Aluminum provides ductile plastic deformation, GFRP reinforcement contributes stiffness and strength, and polyurethane foam supports progressive collapse from the internal core. This hybrid concept is relevant for automotive impact protection because frontal vehicle components must absorb impact energy effectively while maintaining low structural mass. As shown in

Figure 1, the front structural component of a vehicle is one of the main regions designed to absorb impact energy during collision. Therefore, this study represents the frontal impact-absorbing component using a hybrid aluminum/GFRP conical tubular structure filled with polyurethane foam.

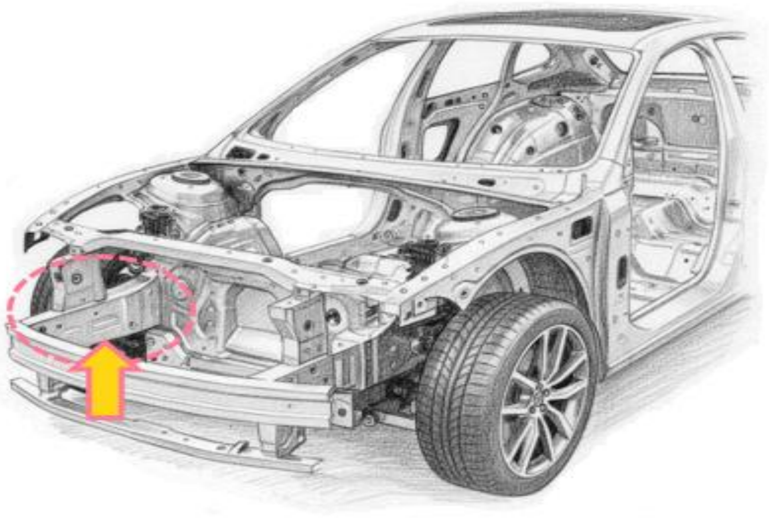

Figure 1. Main frontal vehicle structural component subjected to impact loading.

Finite element analysis (FEA) is widely used to support experimental impact studies because it can simulate deformation, failure response, and energy absorption under controlled boundary conditions (Ahmad et al., 2013). In crashworthiness research, experimental data are commonly used to validate numerical models, while the validated models can then be used to study additional design variables and reduce fabrication cost. Dynamic explicit analysis is commonly applied for impact simulation because it can capture rapid deformation and failure behavior under axial loading. In the present study, the experimental setup and numerical model were designed using similar boundary conditions to compare the impact response of the specimens.

Although previous studies have investigated metallic thin-walled tubes, composite tubes, foam-filled structures, and conical crashworthy components, limited attention has been given to the combined effect of cone angle, GFRP reinforcement, and polyurethane foam filling in thin-walled aluminum conical energy absorbers under axial impact loading. In particular, the comparative crashworthiness performance of different cone angles using the same $[0/90]_2$ GFRP lay-up configuration and different polyurethane foam densities remains insufficiently clarified. This gap is important because cone angle can affect axial load resistance, collapse behavior, energy absorption, and specific energy absorption.

This study aims to investigate the crashworthiness performance of hybrid thin-walled aluminum/GFRP conical energy absorbers filled with polyurethane foam under axial impact loading. Four cone angles, namely 55, 60, 65, and 70°, were examined. The specimens consisted of unreinforced aluminum conical tubes, GFRP-reinforced aluminum conical tubes, and GFRP-reinforced aluminum conical tubes filled with polyurethane foam at densities of 50 and 100 kg/m^3. Experimental impact testing and FEA were conducted to evaluate energy absorption, specific energy absorption, load response, crushing displacement, and failure modes. The novelty of this study lies in its integrated experimental and numerical evaluation of cone angle effects on hybrid aluminum/GFRP conical energy absorbers with polyurethane foam filling, using a consistent $[0/90]_2$ GFRP lay-up and two foam densities. This approach provides a clearer understanding of how cone angle, composite reinforcement, and foam core filling interact to influence crashworthiness performance under axial impact loading.

2. METHODOLOGY

This study combined experimental impact testing and FEA to investigate the crashworthiness performance of hybrid thin-walled aluminum/GFRP conical energy absorbers filled with polyurethane foam. The experimental work was conducted to obtain impact load, crushing displacement, energy absorption, specific energy absorption, and failure behavior. The numerical model was then developed using the same general testing conditions to compare the experimental and simulated impact responses.

2.1. Experimental Impact Testing

The impact test was conducted using a free-falling impact tower machine. The machine consisted of a vertical tower, pulley system, impactor, specimen support, load cell, data logger, and high-speed camera. During testing, a 20 kg impactor was lifted to a height of 2 m and then released freely to strike the upper part of the specimen. The impact response was recorded using a load cell with a maximum load capacity of 50 kN. The impact data were transferred to a GREENTECH GTDL-350 data logger for data acquisition and analysis. A high-speed camera was also used to observe the deformation and failure behavior during impact loading. The theoretical impact velocity was calculated from the drop height and gravitational acceleration. The experimental setup is shown in **Figure 2**.

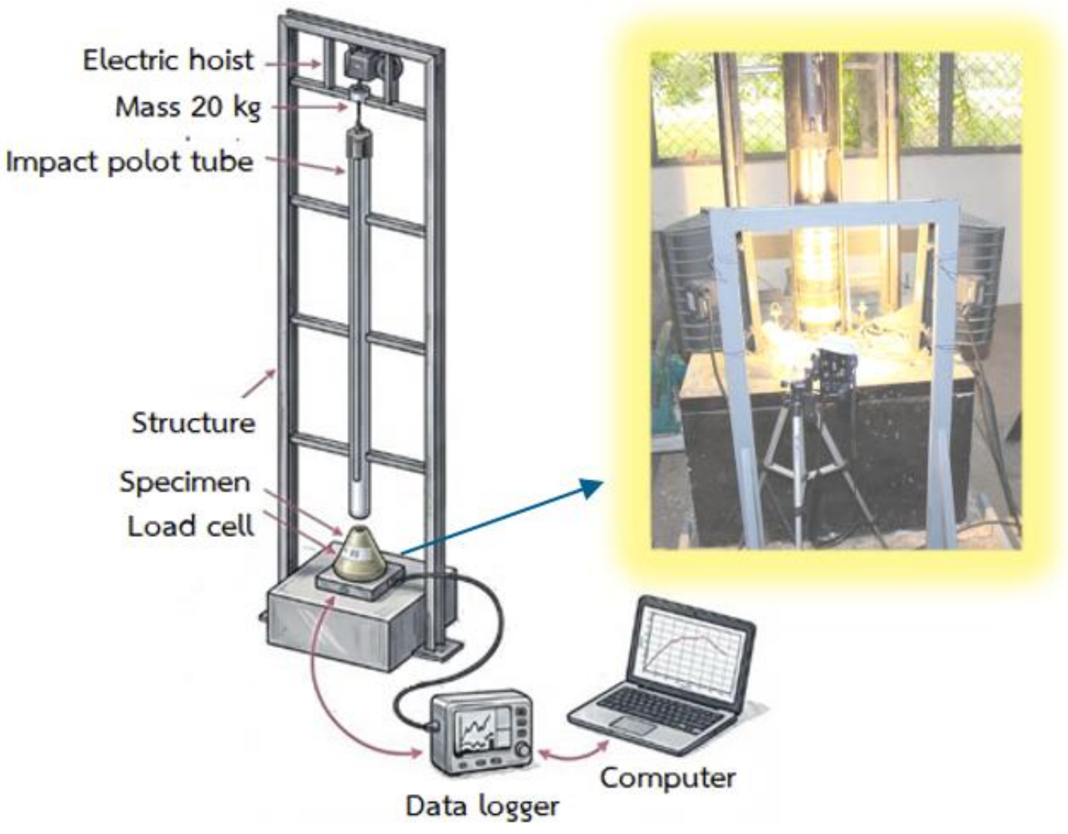

Figure 2. Free-falling impact tower machine and experimental setup.

The impact velocity before contact with the specimen was calculated using Equation (1):

$$V = \sqrt{2gH} \tag{1}$$

where V is the impactor velocity before contact with the specimen, g is gravitational acceleration, and H is the drop height measured from the impactor to the upper edge of the specimen.

2.2. Specimen Design and Fabrication

The specimens were fabricated from thin-walled aluminum sheets formed into conical tubes. Four cone angles were investigated: 55, 60, 65, and 70°. The specimens were divided into four main groups: unreinforced aluminum conical tubes (AL), GFRP-reinforced aluminum conical tubes (AL/G), GFRP-reinforced aluminum conical tubes filled with polyurethane foam at a density of 50 kg/m³ (AL/G/F50), and GFRP-reinforced aluminum conical tubes filled with polyurethane foam at a density of 100 kg/m³ (AL/G/F100). The specimen geometry, cone angle, dimensions, fiber lay-up, and material stacking sequence are shown in **Figure 3**.

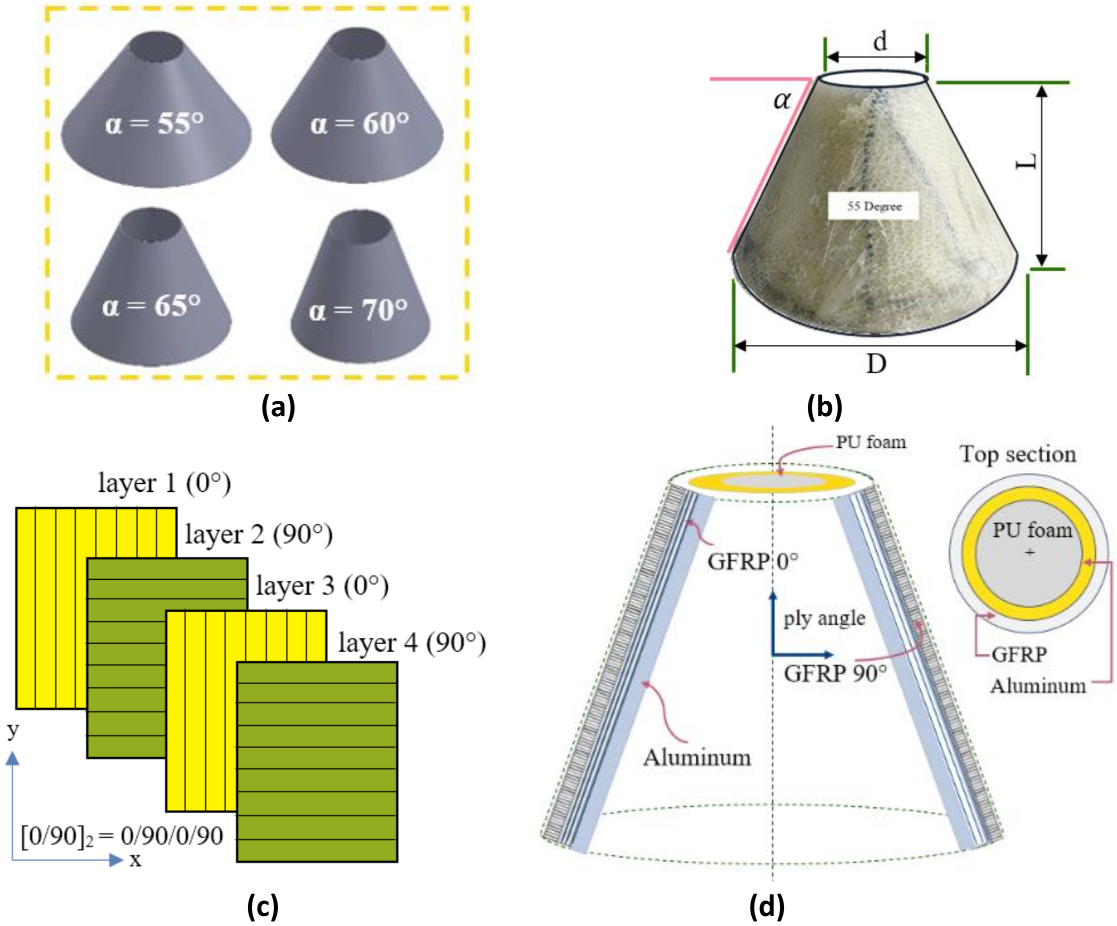

Figure 3. Details of the test specimen fabrication: (a) specimen cone angle, (b) specimen dimensions, (c) glass fiber lay-up configuration, and (d) material stacking sequence.

Unidirectional glass fiber was used as reinforcement because it is relatively inexpensive and provides high strength. The glass fiber layers were arranged in two directions: 0° in the axial direction and 90° in the circumferential direction. Each GFRP-reinforced specimen used a four-layer $[0/90]_2$ lay-up configuration. Polyurethane foam was used as a core filler for selected specimens. In total, 16 specimen configurations were prepared, as presented in **Table 1**.

Table 1. Dimensions and geometric parameters of the specimens.

SPECIMEN CODE	CONE ANGLE (DEGREE)	FOAM DENSITY (kg/m³)	D/d RATIO	HEIGHT (mm)	FIBER PLY ANGLE
AL55	55	Hollow	2.60	100	-
AL60	60	Hollow	2.57	100	-
AL65	65	Hollow	2.46	100	-
AL70	70	Hollow	2.66	100	-
AL55/G	55	Hollow	2.66	100	$[0/90]_2$
AL60/G	60	Hollow	2.63	100	$[0/90]_2$
AL65/G	65	Hollow	2.44	100	$[0/90]_2$
AL70/G	70	Hollow	2.52	100	$[0/90]_2$
AL55/G/F50	55	50	2.67	100	$[0/90]_2$
AL60/G/F50	60	50	2.61	100	$[0/90]_2$
AL65/G/F50	65	50	2.48	100	$[0/90]_2$
AL70/G/F50	70	50	2.41	100	$[0/90]_2$
AL55/G/F100	55	100	2.72	100	$[0/90]_2$
AL60/G/F100	60	100	2.63	100	$[0/90]_2$
AL65/G/F100	65	100	2.52	100	$[0/90]_2$
AL70/G/F100	70	100	2.46	100	$[0/90]_2$

Note: AL = aluminum, G = glass fiber, and F = polyurethane foam.

2.3. Vacuum Infusion Process

The GFRP-reinforced specimens were fabricated using the vacuum infusion process. The main equipment included a vacuum pump, resin storage tank, vacuum tank, vacuum tubes, bagging film, resin distribution mesh, resin absorbent fabric, and release film. The resin and hardener were mixed according to the manufacturer's recommended ratio of 200:70 by weight and stirred until a uniform mixture was obtained. The vacuum pump was then activated to remove air from the bagging film, and the vacuum pressure was adjusted to approximately 0.2 bar. Under vacuum pressure, the resin mixture was drawn into the bagged specimen and penetrated the glass fiber layers. The vacuum infusion process is shown in **Figure 4**.

After resin infusion, the specimens were left to cure for 24-48 h. The demoulding process was conducted by removing the connecting hoses, cutting the vacuum bag, and removing the resin distribution mesh, absorbent fabric, and release film. Examples of the fabricated 55° specimens, including AL55, AL55/G, AL55/G/F50, and AL55/G/F100, are shown in **Figure 5**.

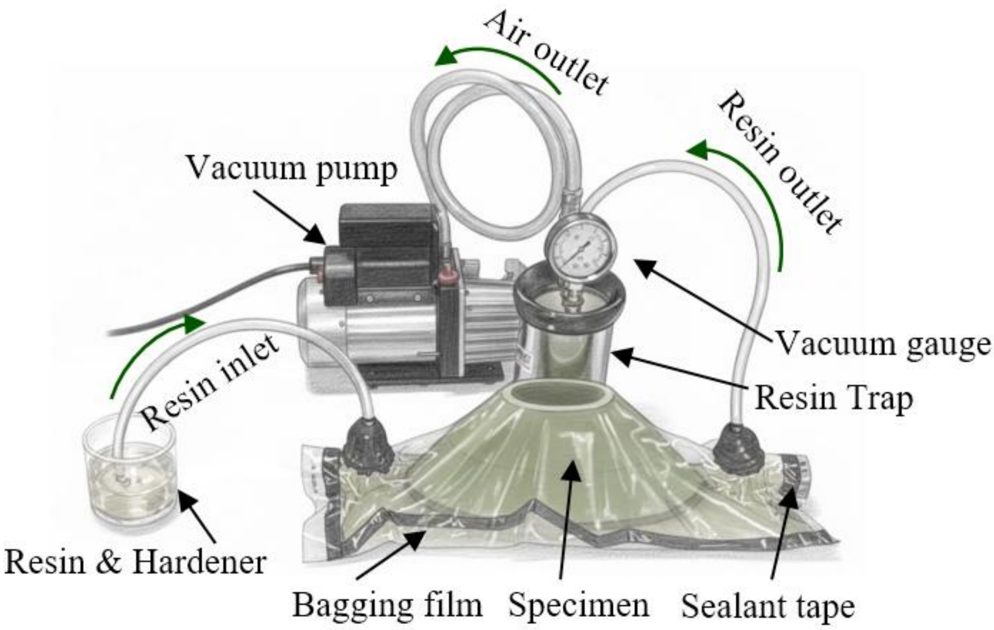

Figure 4. Process and equipment for specimen fabrication using the vacuum infusion process.

(a) AL55 **(b)** AL55/G **(c)** AL55/G/F50 **(d)** AL55/G/F100

Figure 5. Examples of 55° aluminum conical structures reinforced with GFRP composite and filled with polyurethane foam: (a) AL55, (b) AL55/G, (c) AL55/G/F50, and (d) AL55/G/F100.

2.4. Crashworthiness Indicator Parameters

The crashworthiness performance of each specimen was evaluated using impact load, crushing displacement, mean crushing load, energy absorption, and specific energy absorption. The impact load and crushing displacement were obtained from the load-displacement response during impact testing. Energy absorption was calculated from the area under the load-displacement curve. In this study, energy absorption was determined using Equation (2).

$$E_a = P_{\text{mean}} S \quad (2)$$

where Ea is the energy absorption, P_{mean} is the mean crushing load during the collapse process, and S is the crushing displacement.

Specific energy absorption was used to evaluate the energy absorption efficiency relative to structural mass. This parameter is important for lightweight crashworthy structures because an efficient structure should absorb high impact energy while maintaining low mass. Specific energy absorption was calculated using Equation (3) (Onsalung *et al.*, 2014).

$$E_s = \frac{E_a}{m} \quad (3)$$

where *Es* is the specific energy absorption, *Ea* is the energy absorption, and *m* is the mass of the structure.

2.5. Finite Element Analysis

FEA was conducted using ABAQUS to simulate the impact behavior of the conical specimens. The numerical model was developed according to the experimental configuration. The model consisted of three main parts: the upper rigid impactor, the thin-walled aluminum conical specimen, and the lower rigid support plate. The upper impactor was modeled as a rigid body, while the aluminum conical tube was modeled using deformable shell elements. The lower plate was also defined as a rigid body, and a reference node was used to record the impact force during collapse. The finite element model is shown in **Figure 6**.

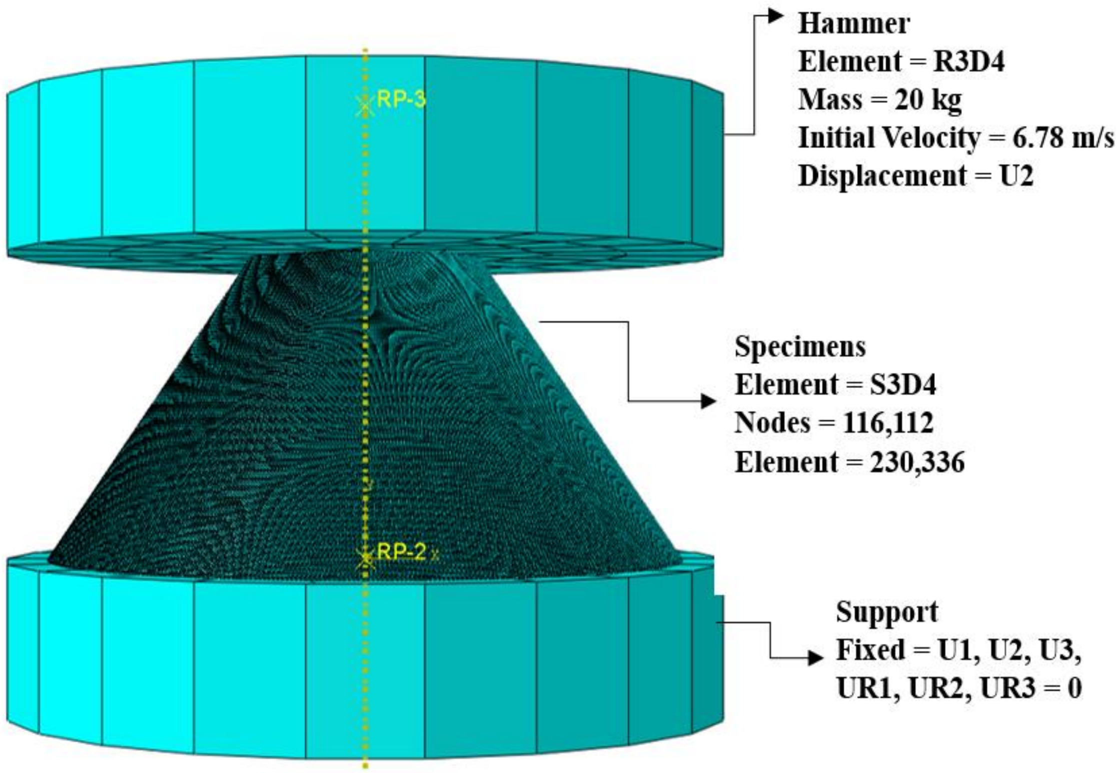

Figure 6. Finite element model of the conical specimen.

The impactor was allowed to move only in the axial direction. The contact interaction between components was defined using hard contact in the normal direction, while the friction coefficient was set to 0.2, based on the literature (Santosa *et al.*, 2000). The fiber orientations were defined at 0 and 90° to represent the axial and circumferential directions of the unidirectional GFRP layers. The definition of fiber orientation is shown in **Figure 7**.

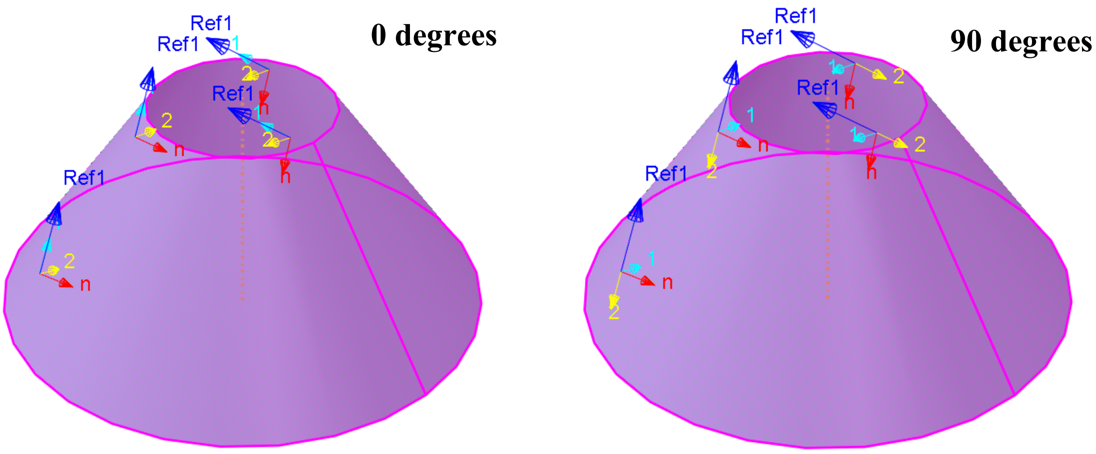

(a) 0° direction **(b)** 90° direction

Figure 7. Definition of fiber orientation: (a) 0° direction and (b) 90° direction.

2.6. Material Properties

The material properties used in the finite element model were obtained from material testing and reference data. The aluminum specimens were tested using an Instron 8801 dynamic universal testing machine at the National Metal and Materials Technology Center (MTEC), Thailand. The tensile test followed ASTM E8 under a quasi-static tensile rate of 10 mm/min. The aluminum material had a density of 2,700 kg/m³, Young's modulus of 42.92 GPa, and Poisson's ratio of 0.33.

Rigid polyurethane foam was used as the core filler. The polyurethane foam was prepared by mixing two liquid components at a 1:1 volume ratio. Compression testing was conducted to obtain the yield stress and hardening behavior required for the numerical model. In ABAQUS, the polyurethane foam was modeled using a crushable foam model with isotropic hardening. The true stress-plastic strain relationships of polyurethane foam and aluminum are presented in **Table 2**.

Table 2. True stress-plastic strain relationships of polyurethane foam and aluminum.

MATERIAL	TRUE STRESS (MPA)	PLASTIC STRAIN
Polyurethane foam, 50 kg/m³	0.727; 0.763; 0.829; 0.952; 1.056; 1.232; 1.662	0.000; 0.052; 0.096; 0.148; 0.191; 0.245; 0.287
Polyurethane foam, 100 kg/m³	2.051; 2.214; 2.306; 2.428; 2.583; 2.860; 3.193	0.000; 0.040; 0.077; 0.113; 0.172; 0.238; 0.295
Aluminum	163.366; 172.847; 184.901; 187.429; 189.133	0.000; 0.008; 0.024; 0.030; 0.032

The GFRP material properties were defined according to the requirements of the damage model. The GFRP was modeled as a unidirectional E-glass fiber/polyester lamina. The mechanical properties were used for the GFRP material (Junchuan and Thinvongpituk, 2020). The strength properties, including tensile, compressive, and shear strengths, are presented in **Table 3**.

Table 3. Properties of unidirectional E-glass fiber/polyester lamina (GFRP).

PROPERTY	DESCRIPTION	VALUE
Density	Density (kg/m³)	1,800
E_{11}	Young's modulus in longitudinal/fiber direction (GPa)	30.75
E_{22}	Young's modulus in transverse direction (GPa)	2.388
G_{12}	In-plane shear modulus (GPa)	6.373
G_{23}	Out-of-plane shear modulus (GPa)	1.056
v_{12}	Poisson's ratio	0.28
X_t	Longitudinal tensile strength (MPa)	721.55
Xc	Longitudinal compressive strength (MPa)	138.11
Y_t	Transverse tensile strength (MPa)	13.78
Yc	Transverse compressive strength (MPa)	13.81
S_{12}	Longitudinal shear strength (MPa)	12.01
S_{23}	Transverse shear strength (MPa)	24.02

2.7. Damage Theory and Failure Evolution

The damage criteria for the GFRP composite in the finite element model were defined based on unidirectional fiber layers arranged in a laminated configuration. Because the GFRP reinforcement was modeled as a composite lamina, damage initiation was evaluated using the Hashin damage initiation criterion. This criterion was selected because it can represent the main failure mechanisms of unidirectional fiber-reinforced composites, including fiber tension, fiber compression, matrix tension, and matrix compression (Hashin, 1980; Hashin and Rotem, 1973).

Damage initiation refers to the onset of stiffness degradation in the composite layer when the stress state reaches a critical condition. In this study, four damage initiation mechanisms were considered, as expressed in Equations (4)-(7).

Fiber tension ($\bar{\sigma}_{11} \geq 0$); $$F_f^t = \left(\frac{\bar{\sigma}_{11}}{X_T}\right)^2 + \alpha\left(\frac{\bar{\tau}_{12}}{S_L}\right)^2 \quad (4)$$

Fiber compression ($\bar{\sigma}_{11} < 0$); $$F_f^c = \left(\frac{\bar{\sigma}_{11}}{X_C}\right)^2 \quad (5)$$

Matrix tension($\bar{\sigma}_{22} \geq 0$); $$F_m^t = \left(\frac{\bar{\sigma}_{22}}{Y_T}\right)^2 + \left(\frac{\bar{\tau}_{12}}{S_L}\right)^2 \quad (6)$$

Matrix compression ($\bar{\sigma}_{22} < 0$); $$F_m^c = \left(\frac{\bar{\sigma}_{22}}{2S_T}\right)^2 + \left[\left(\frac{Y_c}{2S_T}\right)^2 - 1\right]\left(\frac{\bar{\sigma}_{22}}{Y_C}\right)^2 + \left(\frac{\bar{\tau}_{12}}{S_L}\right)^2 \quad (7)$$

where X_T is the longitudinal tensile strength, X_C is the longitudinal compressive strength, Y_T is the transverse tensile strength, Y_C is the transverse compressive strength, S_L is the longitudinal shear strength, and S_T is the transverse shear strength. The stress components used in the criterion represent the effective stress tensor components in the composite material plane.

After damage initiation, the stiffness degradation of the composite material was described using the damaged elasticity matrix. The stiffness degradation model followed the damage mechanics framework for anisotropic fiber composites (Matzenmiller et al., 1995). This approach is suitable for fiber-reinforced composites because these materials generally show elastic-brittle behavior, where damage occurs without significant permanent plastic deformation. Therefore, the reinforcing fibers were assumed to be uniformly aligned, and the material response was calculated using Equation (8).

$$\sigma = C_d \quad (8)$$

where *Cd* is the damaged elasticity matrix. The detailed form of the damaged elasticity matrix is expressed in Equation (9).

$$C_d = \frac{1}{D}\begin{bmatrix} (1\text{-}d_f)E_1 & (1\text{-}d_f)(1\text{-}d_m)\upsilon_{21}E_1 & 0 \\ (1\text{-}d_f)(1\text{-}d_m)\upsilon_{12}E_2 & (1\text{-}d_m)E_2 & 0 \\ 0 & 0 & (1\text{-}d_s)E_3 \end{bmatrix} \quad (9)$$

In this expression, the damage variables represent the current fiber, matrix, and shear damage states. (E_1) is Young's modulus in the fiber direction, (E_2) is Young's modulus perpendicular to the fiber direction, (G) is the shear modulus, and the remaining terms represent the Poisson's ratios used in the composite material model. These parameters were used to define the degradation behavior of the GFRP reinforcement during impact loading.

The numerical model was validated by comparing the simulated load response, crushing displacement, energy absorption, specific energy absorption, and failure characteristics with the experimental results. This validation was used to evaluate whether the finite element model could capture the main crashworthiness behavior of the hybrid aluminum/GFRP conical energy absorbers under axial impact loading.

3. RESULTS AND DISCUSSION

3.1. Load-Time Curve Analysis

Figure 8 shows the experimental and numerical load-time responses of unreinforced aluminum conical structures with cone angles of 55, 60, 65, and 70°. The 70° specimen produced the highest peak load in both the experimental and FEA results. Increasing the cone angle improved the axial load resistance of the aluminum conical structure. The 70° specimen had a geometry closer to a vertical cylindrical form, allowing it to resist axial impact loading more effectively than specimens with smaller cone angles. In contrast, lower cone angles produced lower peak loads because the more inclined geometry generated greater lateral deformation and reduced axial resistance. The maximum load of the aluminum-only specimens was approximately 3.5 kN, and the load decreased as the cone angle decreased.

The load-time behavior of the unreinforced aluminum specimens also shows that the collapse occurred rapidly after the initial peak load. This behavior is typical of thin-walled metallic structures under axial impact, where the initial contact produces a sharp load increase followed by progressive deformation and load reduction. Although aluminum can absorb energy through plastic deformation, the absence of external reinforcement caused the structure to deform more severely. The aluminum-only specimens were more vulnerable to sudden collapse and fragmentation compared with the reinforced specimens.

Figure 9 presents the load-time responses of aluminum conical structures reinforced with GFRP composite. The overall response pattern was similar to that of the unreinforced aluminum specimens, but the reinforced structures showed improved resistance during impact. The specimens sustained the impact load for approximately 0.005 s before the load gradually decreased until collapse was completed. The 70° GFRP-reinforced specimen again produced the highest peak load in both experimental and numerical results. The maximum load was approximately 3 kN. The agreement between the experimental and numerical responses indicates that the finite element model was able to represent the general impact behavior of the GFRP-reinforced conical specimens.

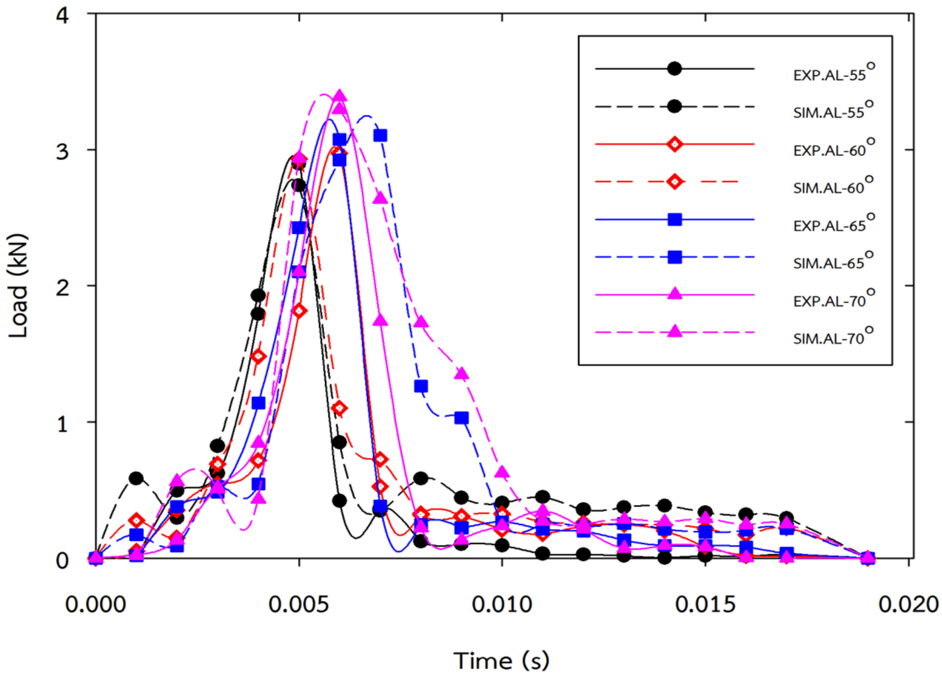

Figure 8. Experimental and numerical load-time responses of aluminum conical structures with cone angles of 55, 60, 65, and 70°.

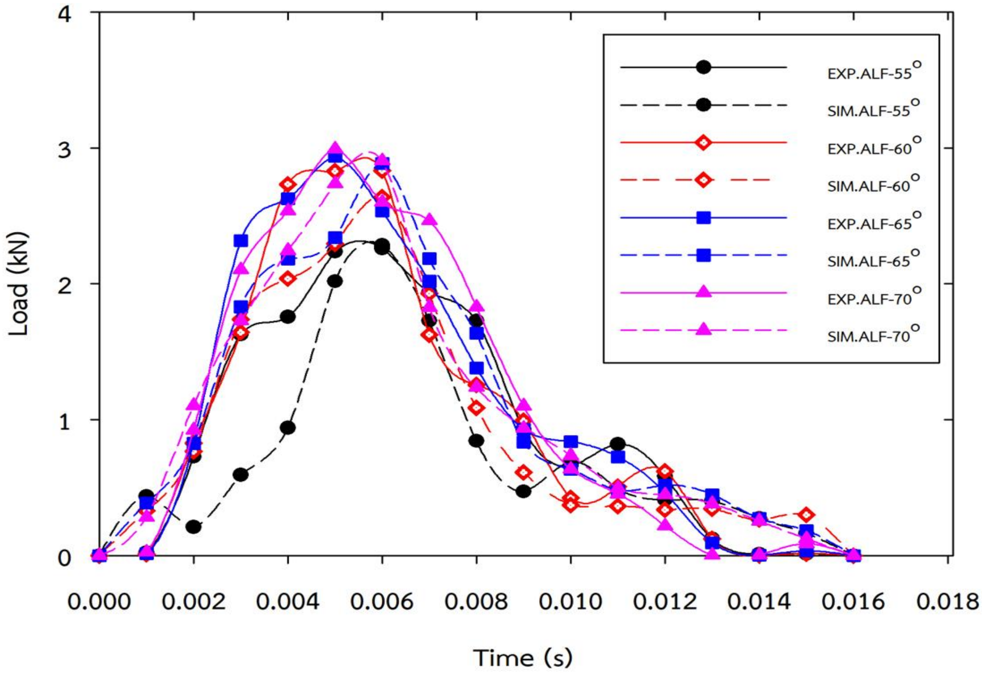

Figure 9. Experimental and numerical load-time responses of aluminum conical structures with cone angles of 55, 60, 65, and 70° reinforced with GFRP composite.

The effect of GFRP reinforcement can be observed from the more controlled load response. The GFRP layer helped delay structural collapse by providing additional stiffness and strength to the aluminum tube. The composite wrapping constrained excessive deformation of the aluminum wall and supported the load-bearing capacity of the structure during the early stage of impact. However, because GFRP composite tends to fail in a brittle manner, the reinforced specimens also experienced damage mechanisms such as cracking, splitting, and delamination during collapse. These mechanisms contributed to energy dissipation and influenced the final failure mode.

Figure 10 shows the load-time responses of GFRP-reinforced aluminum conical structures filled with polyurethane foam at a density of 50 kg/m³. The peak load occurred at approximately 0.003 s. Among this group, the 70° specimen produced the highest peak load, and the numerical result was higher than the experimental result. The peak load was approximately 1.8-2.0 kN. Compared with the unreinforced aluminum specimens and the GFRP-reinforced specimens without foam, the specimens filled with 50 kg/m³ polyurethane foam showed lower peak loads. This reduction is beneficial because a lower peak impact force can reduce the force transmitted to the protected structure or occupant area.

The reduction in peak load after foam filling indicates that polyurethane foam changed the collapse response of the hybrid structure. Instead of producing a sharp and high load peak, the foam-filled specimens showed a more moderated response. The foam core supported the internal wall of the aluminum tube and influenced the collapse pattern by distributing the impact load more gradually. This behavior is important in crashworthy structures because effective energy absorbers should not only absorb high energy but also control the load transmitted during impact.

Figure 11 presents the load-time responses of GFRP-reinforced aluminum conical structures filled with polyurethane foam at a density of 100 kg/m³. The results showed a similar trend to the 50 kg/m³ foam-filled specimens. The experimental and numerical results were generally consistent. For the 70 and 65° specimens, the numerical peak loads were approximately 1.3-1.5 kN. The lowest experimental load was observed in the 55° specimen. Both foam densities reduced the peak load compared with the specimens without foam.

Polyurethane foam filling can help maintain a more appropriate mean load during collapse and reduce sudden impact force. Cone angle, GFRP reinforcement, and polyurethane foam filling strongly affected the impact response of the conical energy absorbers. Increasing the cone angle generally increased the load capacity because the structure became more aligned with the axial loading direction. GFRP reinforcement improved structural resistance and delayed collapse, while polyurethane foam reduced the sudden peak load and promoted a more controlled collapse response. The comparison between experimental and numerical results also shows that the FEA model captured the main trends of the impact behavior, although some differences were observed due to idealized boundary conditions, material definitions, and contact assumptions in the numerical model.

Table 4 summarizes the experimental and numerical load-time responses of all specimen configurations. The comparison shows that the FEA model generally captured the main trend of the experimental load response, although local differences appeared due to boundary conditions, material assumptions, and contact definitions.

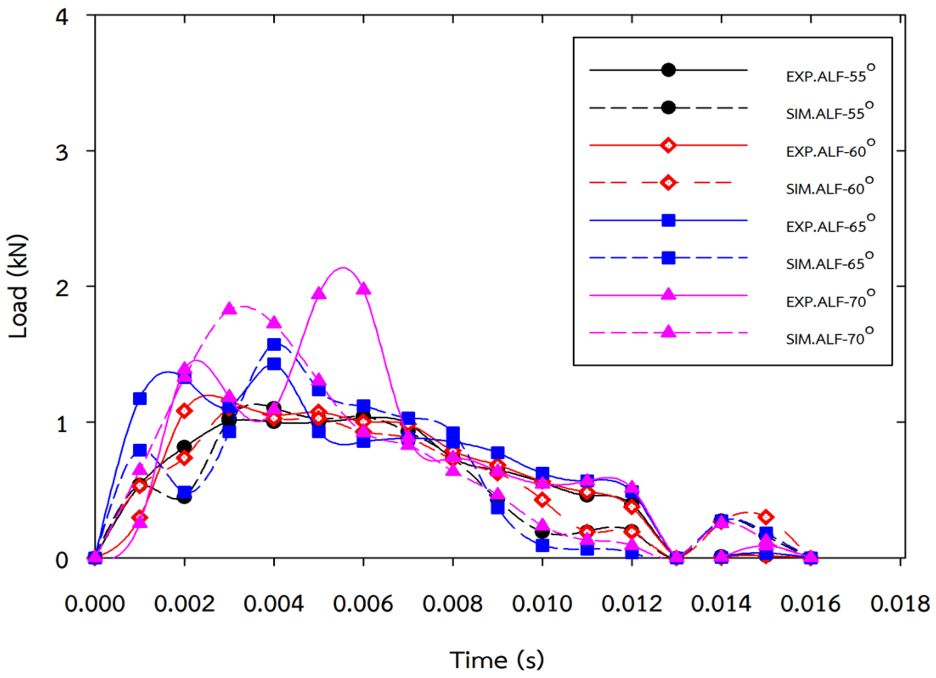

Figure 10. Experimental and numerical load-time responses of aluminum conical structures with cone angles of 55, 60, 65, and 70° reinforced with GFRP composite and filled with polyurethane foam at a density of 50 kg/m³.

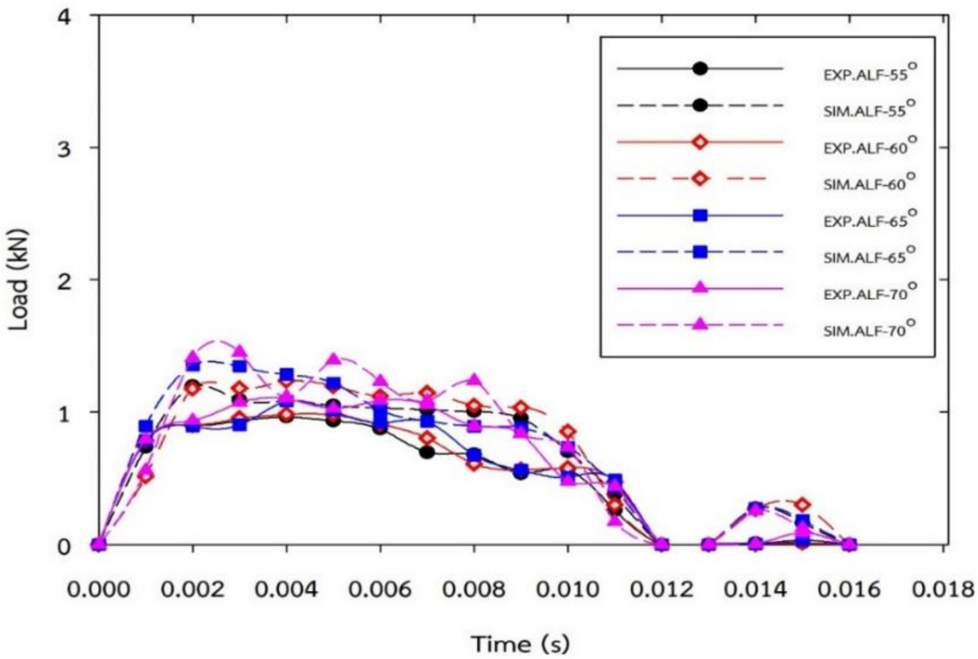

Figure 11. Experimental and numerical load-time responses of aluminum conical structures with cone angles of 55, 60, 65, and 70° reinforced with GFRP composite and filled with polyurethane foam at a density of 100 kg/m³.

Table 4. Comparison of experimental and numerical load-time responses of aluminum conical specimens under impact loading.

SPECIMENS	CONE ANGLE (DEGREE)			
	55°	60°	65°	70°
AL	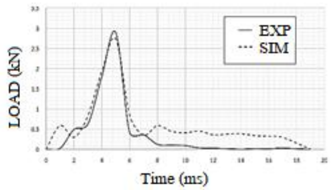	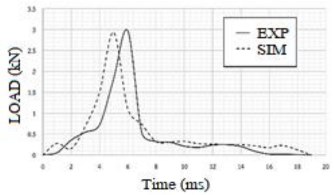	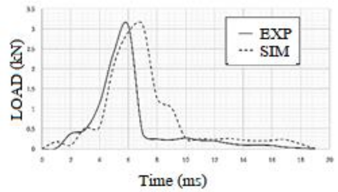	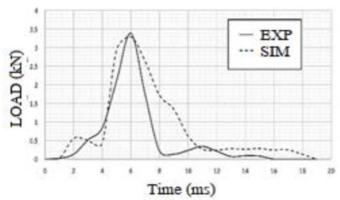
AL/G	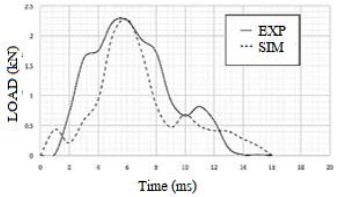	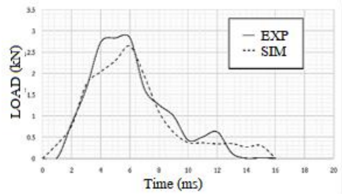	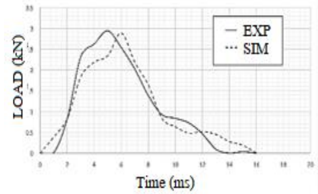	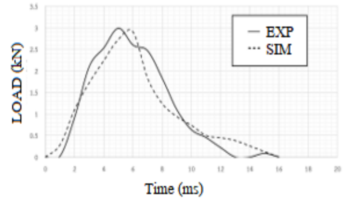
AL/G/F50	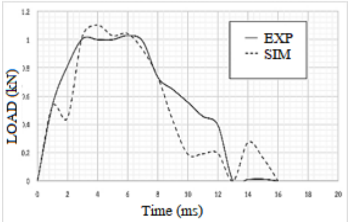	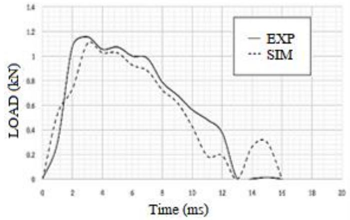	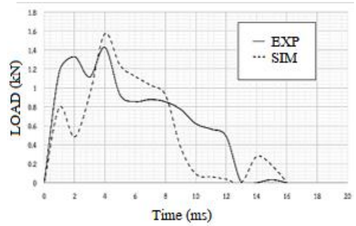	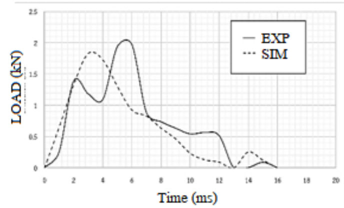
AL/G/F100	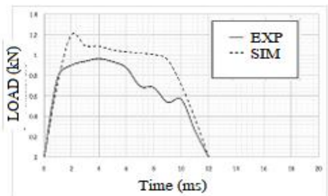	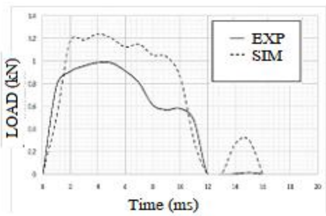	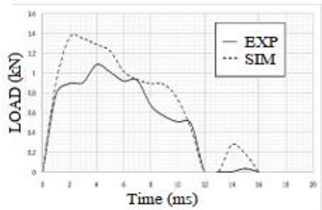	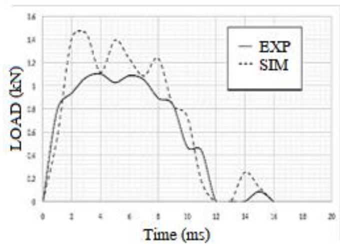

3.2. Crushing Displacement

Figure 12 presents the crushing displacement of all specimen configurations obtained from experimental testing. The results show that unreinforced aluminum conical specimens had greater crushing displacement than the GFRP-reinforced and foam-filled specimens. The aluminum-only specimens showed crushing displacement values of approximately 30-32 mm, whereas the reinforced and foam-filled configurations generally showed values of approximately 27-28 mm. This indicates that GFRP reinforcement and polyurethane foam filling reduced the total deformation of the conical structures during impact loading.

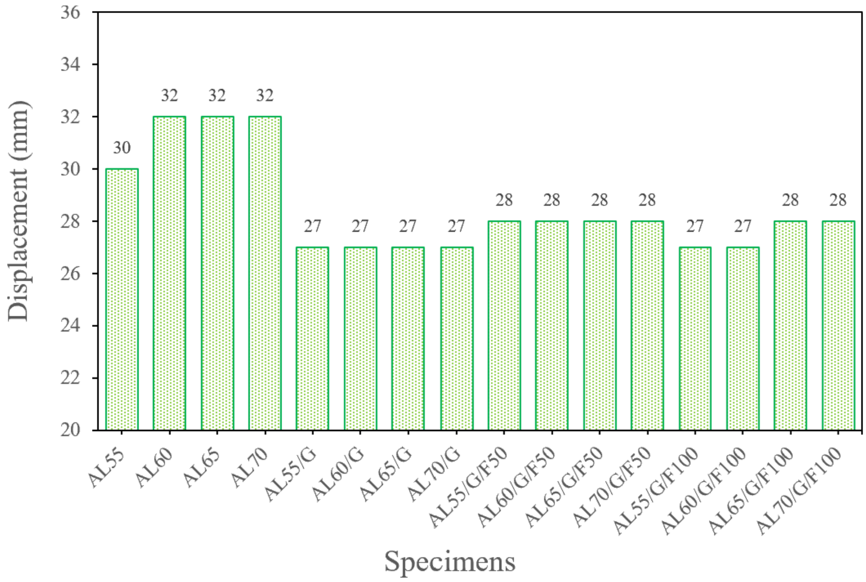

Figure 12. Crushing displacement of all specimen configurations obtained from experimental testing.

The lower crushing displacement in the reinforced and foam-filled specimens indicates that the hybrid structures were more resistant to deformation under axial impact loading. The GFRP wrapping constrained the outward deformation of the aluminum wall, while the polyurethane foam supported the internal space of the conical tube. As a result, the deformation was more controlled and the collapse distance became shorter. However, lower crushing displacement does not necessarily mean lower crashworthiness performance. Energy absorption depends on the combination of sustained load and crushing displacement. Therefore, the load-time response and energy absorption values must be analyzed together to determine the most effective specimen configuration.

The aluminum-only specimens showed larger deformation because the thin-walled aluminum tubes had no external composite reinforcement or internal foam support. Under axial impact, these specimens experienced more severe wall deformation and collapse. In contrast, the GFRP-reinforced specimens showed more limited displacement because the composite layers increased structural stiffness and reduced excessive deformation. The foam-filled specimens also showed controlled crushing because the foam core helped stabilize the collapse process. This indicates that reinforcement and foam filling can improve the structural stability of conical energy absorbers during impact loading.

The crushing displacement values of the GFRP-reinforced and foam-filled specimens were relatively similar, especially for specimens with the same reinforcement and foam density.

Differences in energy absorption among specimen configurations were influenced not only by displacement but also by the load sustained during impact. Therefore, a specimen with slightly lower displacement may still show higher energy absorption if it can maintain a higher mean crushing load. This relationship is important for evaluating lightweight crashworthy structures because the best design should balance deformation control, load stability, and absorbed energy.

3.3. Energy Absorption

Figure 13 presents the energy absorption of unreinforced aluminum conical structures with cone angles of 55, 60, 65, and 70°. Energy absorption increased as the cone angle increased. The 70° specimen achieved the highest energy absorption in both experimental testing and FEA, with values of 17.10 J and 21.82 J, respectively. In contrast, the 55° specimen showed the lowest energy absorption, with values of 11.15 J from the experiment and 15.12 J from FEA. Compared with AL55, AL70 absorbed 53.36% more energy in the experimental result and 44.31% more energy in the FEA result.

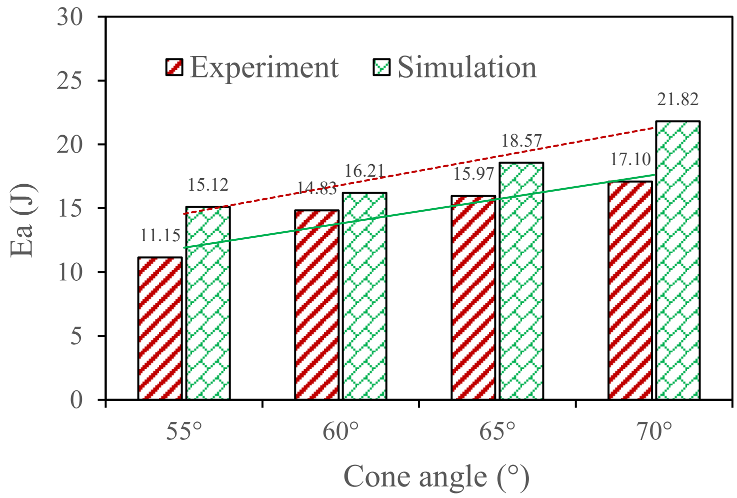

Figure 13. Energy absorption of aluminum conical structures with cone angles of 55, 60, 65, and 70° obtained from experimental testing and FEA.

The increasing energy absorption with cone angle can be explained by the geometry of the conical structure. A larger cone angle produced a structure that was closer to a cylindrical form and more aligned with the axial impact direction. This geometry allowed the specimen to resist the impact load more effectively and absorb more energy during collapse. In contrast, a smaller cone angle created a more inclined wall geometry, which reduced axial load resistance and promoted less effective energy absorption. Therefore, cone angle is a key geometric parameter influencing the crashworthiness performance of aluminum conical energy absorbers.

The FEA results for the aluminum-only specimens were higher than the experimental results, but both methods showed the same trend. This difference may be caused by idealized boundary conditions, simplified material behavior, and assumptions in the numerical contact model. In experimental testing, imperfections in specimen fabrication, local buckling, friction variation, and non-uniform deformation can reduce the measured energy absorption. Nevertheless, the agreement in trend confirms that the FEA model can reasonably represent the influence of cone angle on the energy absorption behavior of unreinforced aluminum conical structures.

Figure 14 shows the energy absorption of aluminum conical structures reinforced with GFRP composite. GFRP reinforcement significantly improved the energy absorption performance compared with unreinforced aluminum specimens. The 70° GFRP-reinforced specimen achieved the highest energy absorption, with 28.55 J from the experiment and 31.80 J from FEA.. The lowest experimental value in this group was observed in AL60/G, with 20.40 J, while its FEA value was 28.20 J. Energy absorption generally increased with cone angle, although AL60/G showed a lower experimental value than expected.

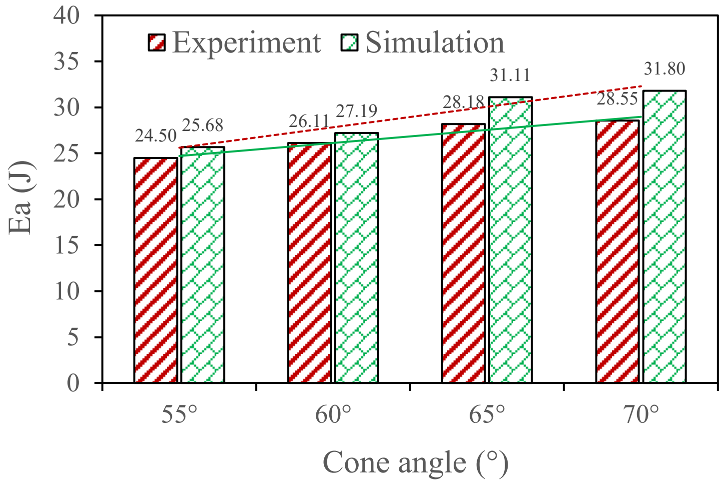

Figure 14. Energy absorption of aluminum conical structures with cone angles of 55, 60, 65, and 70° reinforced with GFRP composite obtained from experimental testing and FEA.

The improvement in energy absorption after GFRP reinforcement shows the beneficial effect of the composite wrapping. The GFRP layers increased the load-bearing capacity of the aluminum conical structure and helped control wall deformation during impact. The composite reinforcement also introduced additional energy dissipation mechanisms, including matrix cracking, fiber damage, delamination, and friction between damaged layers. These mechanisms contributed to higher absorbed energy compared with the unreinforced aluminum specimens. For example, AL70/G absorbed 92.9% more energy than AL70 in the experimental result and 71.89% more energy in the FEA result. GFRP reinforcement is effective for improving the crashworthiness of thin-walled aluminum conical structures.

Although the GFRP-reinforced specimens showed high energy absorption, their behavior was not only controlled by cone angle. The interaction between aluminum deformation and GFRP damage also influenced the final energy absorption value. The lower experimental value of AL60/G may have been caused by local manufacturing variation, non-uniform bonding between aluminum and composite layers, or premature damage during impact. Fabrication quality and interfacial bonding are important factors in hybrid aluminum/GFRP energy absorbers. Therefore, experimental validation remains necessary even when numerical models are used to predict crashworthiness performance.

Figure 15 further confirms the energy absorption trend of GFRP-reinforced aluminum conical structures without foam filling. The GFRP-reinforced specimens achieved higher energy absorption than the unreinforced aluminum specimens, with the 70° cone angle giving the highest value. The experimental values increased from 24.50 J for AL55/G to 28.55 J for AL70/G, while the numerical values increased from 25.68 J to 31.80 J. This confirms that GFRP reinforcement improved the load-bearing capacity and energy dissipation of the conical structures during axial impact loading.

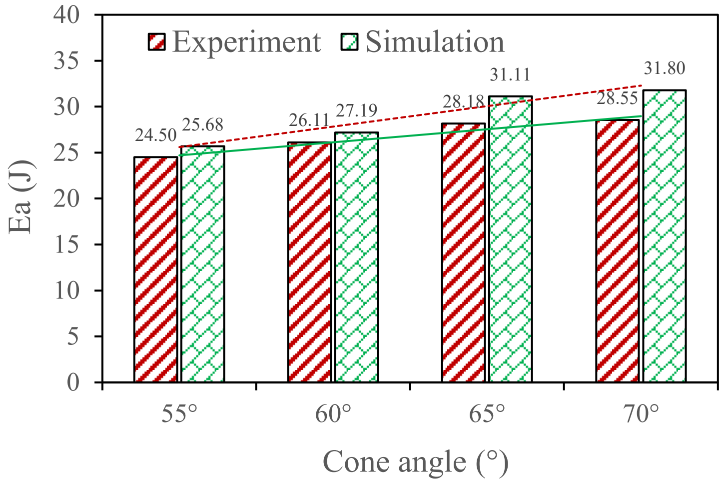

Figure 15. Energy absorption trend of GFRP-reinforced aluminum conical structures with cone angles of 55, 60, 65, and 70° obtained from experimental testing and finite element analysis.

The energy absorption of GFRP-reinforced aluminum conical structures filled with polyurethane foam at a density of 50 kg/m³ was then analyzed based on the experimental and numerical values. The experimental and FEA values were 18.30 J and 22.00 J for AL55/G/F50, 15.70 J and 19.10 J for AL60/G/F50, 19.10 J and 23.40 J for AL65/G/F50, and 18.00 J and 22.40 J for AL70/G/F50, respectively. Unlike the AL/G group, where AL70/G showed the highest energy absorption, the 50 kg/m³ foam-filled group showed the highest value at AL65/G/F50. This indicates that the addition of 50 kg/m³ polyurethane foam changed the collapse mechanism and load distribution inside the conical structure. The foam core supported the inner wall and helped stabilize deformation, but it also reduced the peak load compared with specimens without foam. As a result, the foam-filled specimens did not always absorb more total energy than the GFRP-reinforced specimens without foam.

Figure 16 shows the energy absorption of GFRP-reinforced aluminum conical structures filled with polyurethane foam at a density of 100 kg/m³. The experimental and FEA values were 17.70 J and 18.80 J for AL55/G/F100, 19.70 J and 23.70 J for AL60/G/F100, 18.10 J and 20.90 J for AL65/G/F100, and 21.60 J and 24.20 J for AL70/G/F100, respectively. In this group, AL70/G/F100 achieved the highest energy absorption in both experimental and numerical results. The FEA value was 12.04% higher than the experimental value and 28.72% higher than AL55/G/F100 in the numerical result. The 100 kg/m³ foam-filled specimens showed a clearer increasing trend with cone angle than the 50 kg/m³ foam-filled specimens. Higher-density polyurethane foam provided stronger internal support during axial impact. The foam core helped resist inward wall deformation and contributed to a more stable collapse process. However, the total energy absorption of the foam-filled specimens was still generally lower than that of the GFRP-reinforced specimens without foam. Foam filling did not necessarily increase total absorbed energy in all configurations. Instead, the main advantage of foam filling was related to controlling collapse behavior, reducing sudden peak load, and improving deformation stability.

Increasing foam density tended to improve energy absorption, especially at larger cone angles. The AL70/G/F100 specimen absorbed more energy than AL70/G/F50, indicating that a denser foam core can provide greater support to the conical wall during impact. Nevertheless, the effect of foam density was not as dominant as the effect of GFRP reinforcement. The GFRP-reinforced specimens without foam still showed the highest energy absorption because the composite layers contributed more strongly to load-bearing capacity and energy dissipation during collapse.

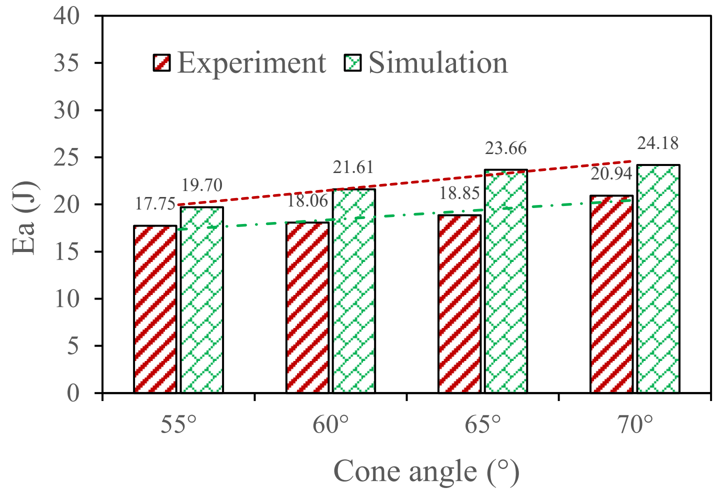

Figure 16. Energy absorption of aluminum conical structures with cone angles of 55, 60, 65, and 70° reinforced with GFRP composite and filled with polyurethane foam at a density of 100 kg/m³.

Figure 17 summarizes the experimental energy absorption of all conical structure configurations under axial impact loading. The AL/G specimens generally achieved the highest energy absorption among all groups. The AL70/G specimen reached the highest value, while the unreinforced aluminum specimens showed the lowest energy absorption. The minimum value was observed in AL55, confirming that a smaller cone angle and the absence of reinforcement reduced crashworthiness performance.

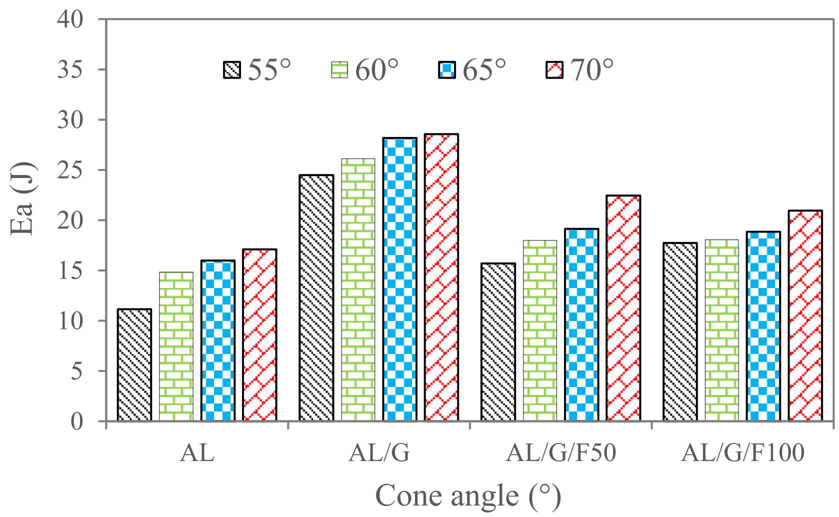

Figure 17. Energy absorption of all conical composite specimen configurations obtained from experimental testing.

GFRP reinforcement had the strongest positive effect on energy absorption. At all cone angles, the AL/G specimens absorbed more energy than the aluminum-only specimens. This improvement can be attributed to the combined deformation of the aluminum tube and the damage mechanisms of the GFRP composite. The aluminum tube absorbed energy through plastic deformation, while the GFRP layer contributed through cracking, delamination, fiber damage, and frictional interaction. Therefore, the hybrid aluminum/GFRP structure provided a more effective energy dissipation mechanism than aluminum alone.

The foam-filled groups showed more complex behavior. Although foam filling helped control peak load and collapse stability, the total energy absorption was lower than that of AL/G specimens. This may be because the polyurethane foam reduced the peak load and changed the deformation mechanism of the structure. In crashworthiness design, this result is important because the best configuration depends on the intended design priority. If the main objective is to maximize total absorbed energy, AL/G specimens, especially AL70/G, are more effective. However, if the objective is to reduce sudden force transmission and promote a more controlled collapse, foam-filled hybrid structures may still be useful.

Cone angle, GFRP reinforcement, and foam filling interact in determining the crashworthiness performance of conical energy absorbers. Increasing cone angle generally increased energy absorption because the structure became more aligned with the axial impact direction. GFRP reinforcement substantially improved the energy absorption capacity of the aluminum conical structure. Polyurethane foam filling modified the collapse process and reduced sudden load response, although it did not always increase total absorbed energy. Therefore, the energy absorption performance should be interpreted together with specific energy absorption and failure behavior to identify the most suitable lightweight crashworthy configuration.

3.4. Specific Energy Absorption

Figure 18 presents the specific energy absorption of conical specimens obtained from experimental testing and FEA at cone angles of 55, 60, 65, and 70°. The results are divided into four groups: unreinforced aluminum specimens, GFRP-reinforced aluminum specimens, GFRP-reinforced aluminum specimens filled with 50 kg/m³ polyurethane foam, and GFRP-reinforced aluminum specimens filled with 100 kg/m³ polyurethane foam.

Figure 18(a) shows the specific energy absorption of unreinforced aluminum conical specimens. AL70 achieved the highest specific energy absorption of 108.24 J/kg, while AL55 showed the lowest value of 71.03 J/kg. The FEA results followed the same trend, with the highest value of 138.10 J/kg for AL70 and the lowest value of 96.33 J/kg for AL55. Increasing cone angle improved not only total energy absorption but also energy absorption efficiency relative to mass. In the experimental results, AL70 showed a 52.39% higher specific energy absorption than AL55.

The increase in specific energy absorption with cone angle can be attributed to improved axial resistance and more effective load transfer during impact. Larger cone angles produced a more cylinder-like geometry, allowing the structure to resist axial loading more efficiently. Although unreinforced aluminum specimens showed lower overall performance than hybrid specimens, geometry alone significantly influences crashworthiness efficiency. Therefore, cone angle should be considered as a primary design parameter in thin-walled conical energy absorbers.

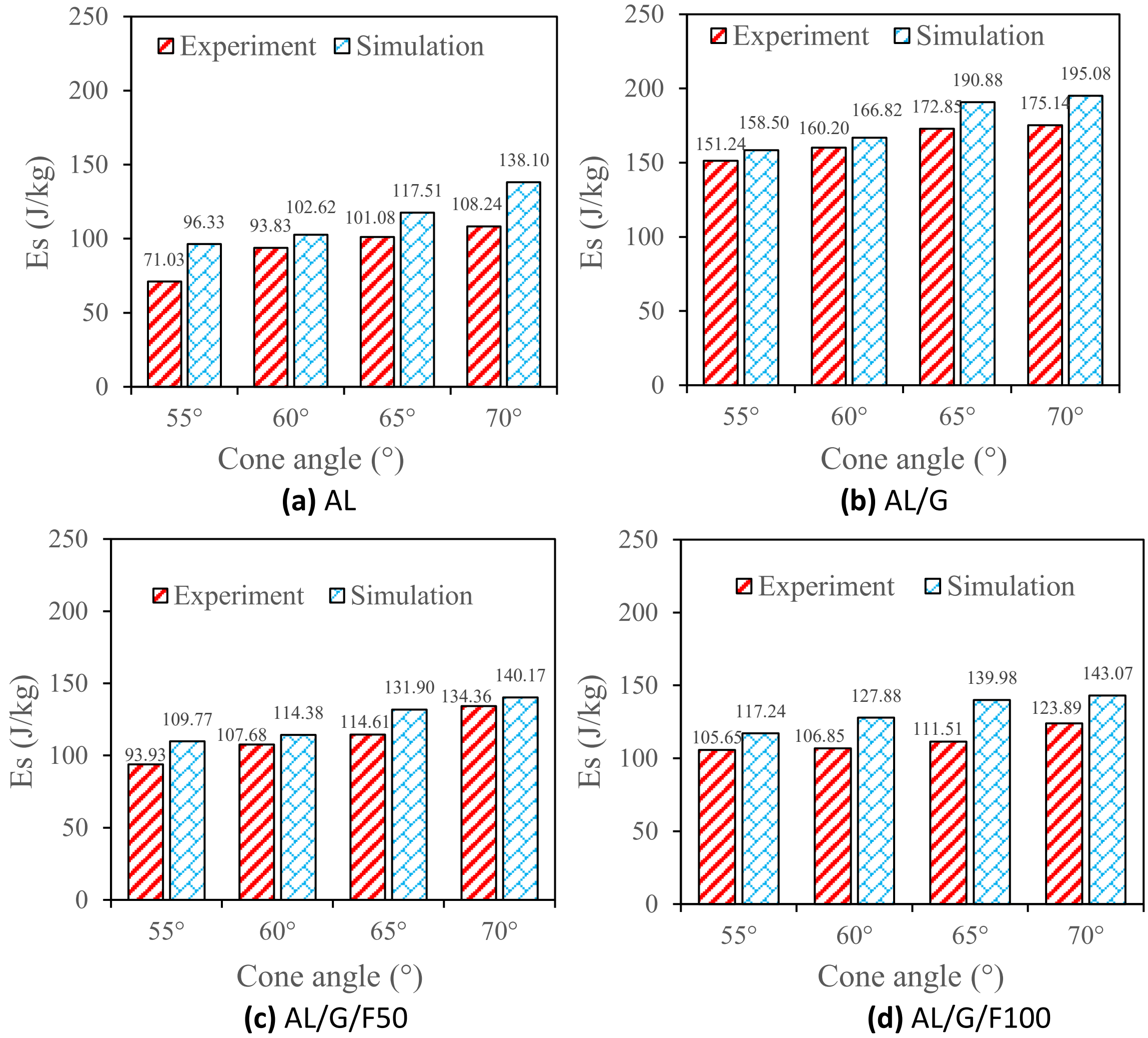

Figure 18. Specific energy absorption of conical specimens obtained from experimental testing and FEA at cone angles of 55, 60, 65, and 70°: (a) AL, (b) AL/G, (c) AL/G/F50, and (d) AL/G/F100.

Figure 18(b) presents the specific energy absorption of GFRP-reinforced aluminum conical structures. The AL70/G specimen achieved the highest experimental value of 175.14 J/kg, while AL55/G showed the lowest value of 151.24 J/kg. The FEA results showed a similar trend, with 195.08 J/kg for AL70/G and 158.50 J/kg for AL55/G. These values were higher than those of the unreinforced aluminum specimens, confirming that GFRP reinforcement improved the lightweight energy absorption efficiency of the conical structures. The improvement in specific energy absorption after GFRP reinforcement indicates that the composite layers increased crashworthiness efficiency without causing an excessive mass penalty. This is important because the objective of lightweight crashworthy structures is not only to absorb more energy but also to absorb energy efficiently relative to structural weight. The GFRP-reinforced specimens provided a better balance between absorbed energy and mass than the unreinforced aluminum specimens. AL/GFRP hybridization is effective for improving the lightweight impact performance of conical energy absorbers.

Figure 18(c) shows the specific energy absorption of GFRP-reinforced aluminum conical structures filled with polyurethane foam at a density of 50 kg/m³. The AL55/G/F50 specimen showed the lowest value, with 93.93 J/kg from the experiment and 109.77 J/kg from FEA. In contrast, AL70/G/F50 showed the highest values, with 140.17 J/kg from the experiment and 134.36 J/kg from FEA. The experimental and numerical results were relatively consistent, and specific energy absorption generally increased with cone angle. The lower specific energy absorption of the 50 kg/m³ foam-filled specimens compared with the AL/G specimens shows that foam filling increased structural mass while not producing a proportional increase in absorbed energy. Although the foam core helped stabilize deformation and reduce sudden peak load, the additional mass reduced energy absorption efficiency. This finding is important for lightweight design because foam filling should be used carefully. If the design priority is maximum specific energy absorption, GFRP reinforcement without foam may be more effective. However, if the design priority is collapse control and peak load reduction, foam filling may still provide practical advantages.

Figure 18(d) presents the specific energy absorption of GFRP-reinforced aluminum conical structures filled with polyurethane foam at a density of 100 kg/m³. The AL70/G/F100 specimen achieved the highest values, with 123.89 J/kg from the experiment and 143.07 J/kg from FEA, while AL55/G/F100 showed the lowest values of 105.65 J/kg and 117.24 J/kg, respectively. Similar to the other specimen groups, the specific energy absorption generally increased with cone angle. The cone angle remained an important geometric factor even when the specimens were reinforced with GFRP and filled with polyurethane foam. The 100 kg/m³ foam-filled specimens showed lower specific energy absorption than the 50 kg/m³ foam-filled specimens at several cone angles. This trend can be explained by the higher mass contribution of the denser foam. Although higher-density foam can provide stronger internal support, the increase in mass may reduce the specific energy absorption value. Therefore, increasing foam density does not automatically improve lightweight crashworthiness efficiency. Foam density must be optimized according to the desired balance between load control, deformation stability, total energy absorption, and mass efficiency.

Figure 19 summarizes the experimental specific energy absorption of all specimen configurations. The unreinforced aluminum conical specimens showed the lowest values, ranging from 71.00 to 108.20 J/kg. In contrast, the GFRP-reinforced specimens showed the highest values, ranging from 151.20 to 175.10 J/kg. Among all configurations, AL70/G achieved the highest specific energy absorption of 175.10 J/kg. The AL70/G configuration provided the most efficient lightweight energy absorption performance in this study. GFRP reinforcement was the most effective factor for improving specific energy absorption. The AL/G group consistently outperformed the unreinforced and foam-filled groups. The energy increase produced by GFRP reinforcement was greater than the mass increase caused by adding the composite layers. In contrast, polyurethane foam filling increased the structural mass and did not always produce a proportional increase in absorbed energy. As a result, the foam-filled configurations showed lower specific energy absorption than the AL/G specimens.

The most efficient configuration depends on the intended crashworthiness function. If the main design target is maximum lightweight energy absorption, the AL70/G configuration is the best option among the tested specimens. However, if the design target includes reducing sudden peak load and promoting controlled collapse, foam-filled configurations may still be considered. Therefore, energy absorption and specific energy absorption should not be interpreted separately. They must be evaluated together with load-time response, crushing displacement, and failure mode to determine the most suitable design for practical impact protection.

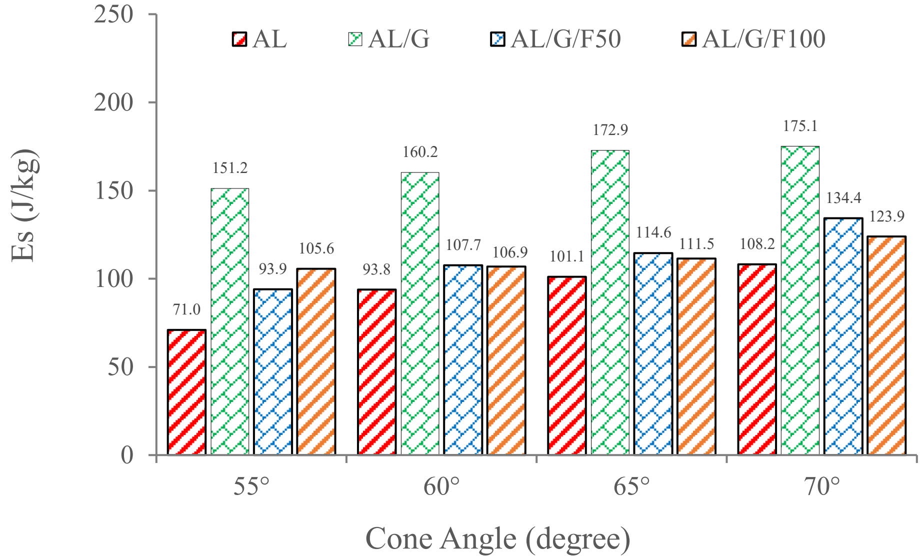

Figure 19. Specific energy absorption of all specimen configurations obtained from experimental testing.

The specific energy absorption results confirm the importance of combining geometry and material reinforcement in the design of hybrid conical energy absorbers. A larger cone angle improved axial resistance and energy absorption efficiency. GFRP reinforcement significantly increased the energy absorbed per unit mass. Polyurethane foam filling improved collapse control but reduced specific energy absorption in several configurations because of the added mass. Therefore, AL70/G can be considered the most effective lightweight crashworthy configuration in this study because it achieved the highest energy absorption and specific energy absorption under axial impact loading.

3.5. Failure Modes of the Specimens

Figure 20 shows the progressive damage of a conical specimen during impact loading. The figure illustrates how the specimen deformed after contact with the impactor and how the collapse developed during the impact process. Progressive damage is desirable in crashworthy structures because it allows the structure to absorb energy gradually rather than failing suddenly. In the present study, different specimen configurations showed different collapse patterns depending on reinforcement and foam filling.

Figure 20. Progressive damage of the conical specimen during impact loading.

The experimental testing and FEA showed several failure patterns after complete specimen collapse. For the composite-reinforced specimens, four main failure modes were identified: splitting with outward splaying, splitting, crushing, and fragmentation. These failure modes are summarized in **Table 5**. The impact response of the hybrid conical structures was not controlled by one single mechanism. Instead, the final damage pattern depended on how the aluminum tube, GFRP reinforcement, and polyurethane foam interacted during axial compression.

Splitting with outward splaying occurred when the specimen wall showed inward crushing combined with outward spreading of the composite layers. This failure mode was associated with the interaction between the 0° and 90° fiber orientations. The 0° layers were aligned with the axial loading direction and therefore carried a major part of the impact load. When the axial load increased, these fibers experienced buckling and local damage. At the same time, the 90° layers constrained the axial fibers and promoted interlaminar separation. This mechanism caused the wall to split and splay outward during crushing.

The second failure mode was splitting. This failure was mainly observed in specimens with smaller cone angles, especially in the 55° group. The smaller cone angle created a more inclined wall geometry, which changed the internal load path during impact. Under axial compression, the inclined structure produced a combination of axial and shear effects. The 0° fibers resisted the inclined internal load, while the 90° fibers constrained the deformation in the circumferential direction. This interaction generated splitting along the specimen wall. Compared with controlled crushing, splitting indicates less stable collapse because the structural wall separated more clearly during impact.

The third failure mode was crushing. This mode was generally observed in several foam-filled specimens and was considered more favorable for energy absorption. In this mode, the specimen collapsed in a more controlled manner rather than breaking into separate fragments. The 0° layers carried the axial load, while the 90° layers constrained deformation and helped maintain the tubular shape. Although delamination and cracking occurred between layers, the laminated thickness and foam core helped limit severe fracture. As a result, crushing failure allowed the structure to absorb impact energy through progressive deformation. Specimens showing controlled crushing generally demonstrated better crashworthiness behavior than those showing severe fragmentation.

The fourth failure mode was fragmentation. This mode occurred mainly in the unreinforced aluminum conical specimens. Without GFRP wrapping or polyurethane foam filling, the aluminum structure had lower resistance to impact damage. During axial loading, the thin-walled aluminum tube experienced severe deformation and fractured into smaller fragments. Fragmentation is not desirable in crashworthy structures because it indicates unstable collapse and limited structural integrity after impact. This behavior explains why the unreinforced aluminum specimens showed lower energy absorption and specific energy absorption than the reinforced specimens.

Table 6 compares the failure characteristics of the conical aluminum structures obtained from experimental testing and FEA. The unreinforced aluminum specimens experienced the most severe damage under axial impact loading. These specimens showed crushing and fragmentation because the aluminum wall alone could not sufficiently control the collapse process. In contrast, the AL/G specimens showed more controlled damage because the GFRP composite layers reinforced the aluminum tube and improved impact resistance. The GFRP wrapping reduced excessive wall deformation and helped maintain the structural shape during impact.

Table 5. Failure modes of the specimens obtained from experimental testing.

FAILURE MODE	SPECIMEN EXAMPLE	SPECIMENS SHOWING THIS FAILURE MODE
Splitting with outward splaying	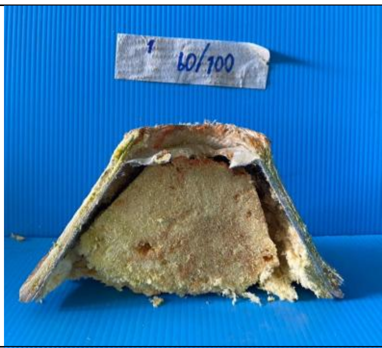	1. AL60/G/F100
Splitting		1. AL55/G/F100
Crushing	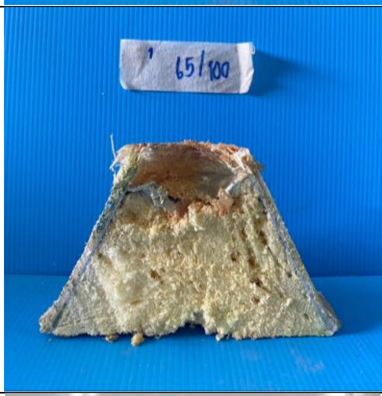	1. AL65/G/F100 2. AL70/G/F100 3. AL55/G/F50 4. AL60/G/F50 5. AL70/G/F50
Fragmentation		1.AL55^{o} 2.AL60^{o} 3.AL65^{o} 4.AL70^{o}

For the AL/G/F50 and AL/G/F100 specimens, the final failure mode was also dominated by crushing. The aluminum tube collapsed under axial impact, while the GFRP composite showed minor cracking and delamination. The polyurethane foam supported the internal core and helped the structure deform progressively during impact. This internal support reduced sudden collapse and promoted more stable deformation. Therefore, foam-filled specimens showed better collapse control than unreinforced aluminum specimens, even though their total energy absorption and specific energy absorption were lower than those of the AL/G specimens in several cases.

The comparison between experimental and numerical failure characteristics indicates that the finite element model captured the main deformation trends of the specimens. The model was able to represent the different responses of aluminum-only, GFRP-reinforced, and foam-filled configurations. However, some differences between experimental and FEA results are expected because experimental specimens may contain fabrication imperfections, uneven bonding, local geometric variation, and non-uniform material distribution. In contrast, the numerical model uses idealized geometry, material properties, contact conditions, and boundary assumptions. These differences can affect the predicted load response, energy absorption, and local failure pattern.

The failure mode analysis supports the quantitative results from load-time response, energy absorption, and specific energy absorption. The unreinforced aluminum specimens showed the lowest crashworthiness performance because they experienced severe deformation and fragmentation. The GFRP-reinforced specimens showed the highest energy absorption and specific energy absorption because the composite wrapping improved structural resistance and introduced additional energy dissipation mechanisms. The foam-filled specimens showed more controlled crushing and lower peak load, although the added foam mass reduced specific energy absorption in several configurations.

The AL70/G configuration provided the best overall performance in this study. This specimen achieved the highest energy absorption and specific energy absorption while maintaining effective structural resistance under axial impact loading. The 70° cone angle improved axial load resistance because the structure was closer to a cylindrical geometry. The GFRP reinforcement further increased the ability of the aluminum tube to resist collapse and dissipate energy. Although polyurethane foam improved collapse stability, the foam-filled specimens did not outperform AL70/G in total energy absorption or specific energy absorption.

Hybrid aluminum/GFRP conical energy absorbers are promising for lightweight crashworthy applications. Cone angle should be carefully selected because it affects load resistance, deformation behavior, and energy absorption efficiency. GFRP reinforcement is highly effective for improving crashworthiness performance, especially when combined with a larger cone angle. Polyurethane foam filling can be useful when the design objective is to reduce sudden peak load and promote controlled crushing. However, foam density and added mass must be optimized to avoid reducing lightweight efficiency.

The crashworthiness performance of hybrid thin-walled aluminum/GFRP conical energy absorbers depends on the interaction among geometry, reinforcement, foam filling, and failure mechanism. Experimental testing and FEA are complementary methods for evaluating impact behavior. Experimental testing provides direct evidence of actual collapse and failure, while FEA helps explain deformation trends and compare structural responses under controlled conditions. The agreement between experimental and numerical trends strengthens the conclusion that cone angle and GFRP reinforcement are key factors controlling the energy absorption performance of the proposed hybrid conical energy absorbers.

Table 6. Failure characteristics of the conical aluminum structures obtained from experimental testing and FEA.

SPECIMENS	**CONE ANGLE (DEGREE)**			
	55°	**60°**	**65°**	**70°**
AL				
				
AL/G				
				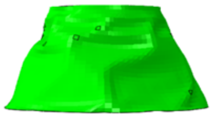
AL/G/F50				
				
AL/G/F100				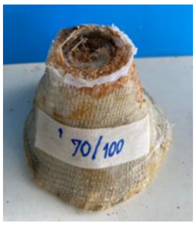
	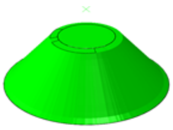			

4. CONCLUSION

This study investigated the crashworthiness performance of hybrid thin-walled aluminum/GFRP conical energy absorbers filled with polyurethane foam under axial impact loading. Experimental testing and FEA showed that cone angle, GFRP reinforcement, and foam filling strongly influenced load response, deformation, energy absorption, and failure behavior. The AL70/G configuration achieved the best performance, providing the highest energy absorption and specific energy absorption. GFRP reinforcement improved structural resistance and energy dissipation, while polyurethane foam reduced sudden peak load and promoted controlled crushing. Cone angle optimization and GFRP reinforcement are effective strategies for lightweight crashworthy energy absorber design.

5. ACKNOWLEDGMENTS

We would like to express their sincere gratitude to Rajamangala University of Technology Isan for providing the research facilities, experimental equipment, and instruments necessary for conducting this study.

7. AUTHORS' NOTE

The authors declare that there is no conflict of interest regarding the publication of this article. The authors confirmed that the paper was free of plagiarism.

8. REFERENCES

Ahmad, M., Ismail, K. A., and Mat, F. (2013). Convergence of finite element model for crushing of a conical thin-walled tube. *Procedia Engineering, 53*, 586-593.

Ataabadi, P. B., Karagiozova, D., and Alves, M. (2019). Crushing and energy absorption mechanisms of carbon fiber-epoxy tubes under axial impact. *International Journal of Impact Engineering, 131*, 174-189.

Gan, N., Feng, Y., Yin, H., Wen, G., Wang, D., and Huang, X. (2016). Quasi-static axial crushing experiment study of foam-filled CFRP and aluminum alloy thin-walled structures. *Composite Structures, 157*, 303-319.

Goel, M. D. (2015). Deformation, energy absorption and crushing behavior of single-, double- and multi-wall foam filled square and circular tubes. *Thin-Walled Structures, 90*, 1-11.

Gupta, N. K., Sheriff, N. M., and Velmurugan, R. (2008). Analysis of collapse behaviour of combined geometry metallic shells under axial impact. *International Journal of Impact Engineering, 35*(8), 731-741.

Hall, I. W., Guden, M., and Claar, T. D. (2002). Transverse and longitudinal crushing of aluminum-foam filled tubes. *Scripta Materialia, 46*(7), 513-518.

Hanssen, A. G., Langseth, M., and Hopperstad, O. S. (2000). Static and dynamic crushing of square aluminium extrusions with aluminium foam filler. *International Journal of Impact Engineering, 24*(4), 347-383.

Hashin, Z. (1980). Failure criteria for unidirectional fiber composites. *Journal of Applied Mechanics, 47*(2), 329-334.

Hashin, Z., and Rotem, A. (1973). A fatigue failure criterion for fiber reinforced materials. *Journal of Composite Materials, 7*(4), 448-464.

Junchuan, V., and Thinvongpituk, C. (2020). The influence of fiber orientation and stacking sequence on the crush behavior of hybrid AL/GFRP tubes under axial impact. *Materials Transactions, 61*(7), 1322-1331.

Liu, W., Lin, Z., Wang, N., and Deng, X. (2016). Dynamic performances of thin-walled tubes with star-shaped cross section under axial impact. *Thin-Walled Structures, 100*, 25-37.

Matzenmiller, A., Lubliner, J., and Taylor, R. (1995). A constitutive model for anisotropic damage in fiber-composites. *Mechanics of Materials, 20*, 125-152.

Mirfendereski, L., Salimi, M., and Ziaei-Rad, S. (2008). Parametric study and numerical analysis of empty and foam-filled thin-walled tubes under static and dynamic loadings. *International Journal of Mechanical Sciences, 50*(6), 1042-1057.

Nandiyanto, A. B. D., Al Husaeni, D. N., Ragadhita, R., Fiandini, M., Al Husaeni, D. F., and Aziz, M. (2022). Resin matrix composition on the performance of brake pads made from durian seeds: From computational bibliometric literature analysis to experiment. *Automotive Experiences*, *5*(3), 328-342.

Onsalung, N., Thinvongpituk, C., and Pianthong, K. (2014). Impact response of circular aluminum tube filled with polyurethane foam. *Materials Transactions, 55*(1), 207-215.

Ozturk, U. E., and Anlas, G. (2011). Finite element analysis of expanded polystyrene foam under multiple compressive loading and unloading. *Materials and Design, 32*(2), 773-780.

Qi, C., Yang, S., and Dong, F. (2012). Crushing analysis and multiobjective crashworthiness optimization of tapered square tubes under oblique impact loading. *Thin-Walled Structures, 59*, 103-119.

Santosa, S. P., Wierzbicki, T., Hanssen, A. G., and Langseth, M. (2000). Experimental and numerical studies of foam-filled sections. *International Journal of Impact Engineering, 24*(5), 509-534.

Wang, L., Zhong, X., Zhao, C., and Zhang, T. (2023). Energy absorption investigation of SFRFC-filled double circular tubes under quasi-static compression and low velocity impact loading. *Construction and Building Materials, 397*, 132217.

Wu, F., Chen, Y., Zhao, S., Hong, Y., Zhang, Z., and Zheng, S. (2023). Mechanical properties and energy absorption of composite bio-inspired multi-cell tubes. *Thin-Walled Structures, 184*, 110451.

Yalçın, M. M., and Genel, K. (2019). On the axial deformation characteristic of PVC foam-filled circular aluminium tube: Effect of radially-graded foam filling. *Thin-Walled Structures, 144*, 106335.

Zarei, H. R., and Kröger, M. (2006). Multiobjective crashworthiness optimization of circular aluminum tubes. *Thin-Walled Structures, 44*(3), 301-308.